Three Component Complex Langmuir – Blodgett Films of Water Soluble Eosin Y With Dodecyl Trimethyl Ammonium Bromide and Stearic Acid

SANTANU CHAKRABORTY, D. BHATTACHARJEE and SYED ARSHAD HUSSAIN*

Department of Physics, Tripura University, Suryamaninagar-799 022, Tripura, India

Abstract — In the present communication we report the formation of nano dimensional complex films of eosin Y (EY), stearic acid (SA) and dodecyl trimethyl ammonium bromide (DTAB) using Langmuir - Blodgett (LB) technique. By spreading SA onto the DTAB - EY mixed aqueous sub phase a complex monolayer of SA-DTAB-EY was formed. The adsorption kinetics in the complex monolayer was investigated by recording increase in surface pressure with time (π–t) graph at air - water interface. Initially the (π–t) graph shows steep rise and becomes flat at the end of the adsorption kinetics. More than 300 minutes were required to complete the adsorption process. In situ Brewster Angle Microscopy investigation gives compelling visual evidence of complex Langmuir monolayer formation at air-water interface. After transfer onto solid substrate the films were characterized by UV-Vis absorption and Atomic Force Microscopy (AFM). In the complex LB films the EY absorption bands were shifted and broadened with respect to pure EY solution and microcrystal spectrum due to the formation of nano dimensional aggregates. This was also supported by AFM investigations of the complex LB films.

Keywords : *Langmuir - Blodgett films, reaction-kinetics, complex film, eosin Y, adsorption, uv-vis absorption, AFM, nano-aggregates.*

INTRODUCTION

Langmuir – Blodgett (LB) films is perhaps the oldest and most useful method to organize molecules in two dimensions [1–3]. The versatility of the method is that it

*Corresponding author. E-mail : sa_h153@hotmail.com; sah.phy@tripurauniv.in, Phone : +91 3812379119 (O), Fax : +91 3812374802 (O)

can be applied to assemble different kind of materials starting from organic, metallorganic, and polymeric compounds to nano-particles [3–4]. The organization of such molecules and the monolayer characteristics can be controlled by changing various film deposition parameters [3–5]. Potentially using this technique one can achieve excellent control of the assembly process that converts the organization of the molecules from a disordered state into a well ordered solid state through the formation of interfacially confined, two dimensional ordered arrangements. This types of films have potential applications in sensors, optoelectronic and microelectronic devices [3–7]. Now scientists are aiming for molecular electronics. LB film may be one of the best fitted techniques to realize the molecular electronics [6, 8]. Therefore, it is necessary to study different molecules possessing interesting spectroscopic and electrical properties, assembled onto LB films in order to explore their possible device applications.

Amphiphilic molecules are ideally suited for LB technique [3]. Also the water soluble surfactants which form micelle are amphiphilic and can be assembled on to ultrathin films using LB technique. However, water soluble materials which do not form micelle can also be assembled onto ultra thin films using LB technique [9–16]. Recent studies reveal that it is possible to adsorb the water soluble material onto a preformed amphiphile monolayer by electrostatic interaction [9–11]. Studies of the interaction of water soluble materials in the aqueous sub phase with Langmuir films of insoluble amphiphile are important to understand the foam and emulsion stability and the relation between monolayer structure and the properties of deposited Langmuir-Blodgett (LB) films [17–19]. Adsorption at interface by electrostatic interaction plays an important role in many biological and technical processes, such as chromatography, adhesion, [20] stabilization of colloidal particles [21] and biocompatibility of artificial organs in medicine [22]. Monitoring the changes on adsorption of a sample from a solution brought into the contact of a preformed amphiphile monolayer, may allow obtaining information about the dynamics of the adsorption process. Certain new properties may come up in such complex multi-component films which were not found in the constituent single component films. Also by choosing proper structure of the amphiphile and the surface pressure applied to the monolayer the charge density and charge mobility can be adjusted. In particular, they exhibit interesting solid-state morphologies due to the separation of the ionic sites and the hydrophobic parts [23–24] and have found applications in surface coatings, drug release systems, etc [23, 25].

Here we report the successful incorporation of a water soluble flurophore eosin Y (EY) doped into DTAB molecules, to the preformed stearic acid (SA) monolayer

at the air–water interface. The resulting complex monolayer was transferred onto solid substrates at desired surface pressure to form mono and multilayered LB films.

Eosin Y is a xanthene dye with interesting photophysical properties. It absorbs light in the visible region of the electromagnetic spectrum. This property of EY makes it a useful candidate for photosensitizers. It was observed that EY is efficient photosensitizers to initiate the cross-linking of proteins [26]. It is also used for dye-sensitized solar cell applications [27–28]. EY is used for the successful FRET Enhancement in Multilayer Core-Shell nano-particles [29].

For photovoltaic application it is important to make electrode with large surface area with uniform thickness. So far in the most cases cast film or spin coated film of EY were used. However, the efficiency may be increased if EY is used in the form of ultra thin films with large surface area and desired thickness. LB technique is probably the best suitable candidate to make uniform ultra thin film with desired thickness. To the best of our knowledge EY has never been studied in LB technique. Therefore, it was felt that incorporation of EY in the restricted geometry of LB films might reveal new features.

EXPERIMENTAL

The materials eosin Y (EY), dodecyl trimethyl ammonium bromide (DTAB) and stearic acid (SA), all were purchased from Sigma-Aldrich chem. Co., USA and were used as received. Working solutions were prepared by dissolving EY and DTAB in ultrapure Millipore water and SA in HPLC grade chloroform.

Monitoring the increase in surface pressure with time (π–t curve) as well as LB film deposition was done by using a typical Langmuir - Blodgett (LB) film deposition instrument (Apex 2000C, India). Initially the LB trough was filled with pure water or mixture of aqueous solution of DTAB (concentration = 10^{-6} M) and EY (concentration = 10^{-6} M) at different volume ratios. 80 μl of chloroform solution of SA (0.5 mg/ml) were spread on the trough to form a SA monolayer on the surface. The barrier was adjusted such that the surface pressure remains close to zero. After that the barrier was kept fixed and corresponding increase in surface pressure with time was recorded using a Wilhelmy arrangement described elsewhere [3, 5].

All the experiments were done at ambient condition in a closed room whose temperature was maintained at 25°C using air condition system.

For spectroscopic measurement LB films were transferred onto clean quartz substrate after the completion of the reaction kinetics and for AFM measurement a cleaned silicon wafer substrate was used for film deposition using standard LB film

deposition technique [3, 5]. The deposition speed was maintained at 5 mm/min.

Microcrystal film of EY was prepared by spreading few drops of dilute EY solution onto a clean quartz substrate by a micro syringe and allowing them to spread throughout the substrate surface. After evaporation of the solvent, a cast film was obtained, which actually contained the microcrystal of EY.

Brewster angle microscopy (BAM) imaging was recorded using an NFT (Göttingen, Germany) Mini BAM. The polarizer and analyzer were set to p-polarization, and the incoming laser light (688 nm, 30 mW) was limited to an angle of incidence of 52^0–54^0 (Brewster angle for aqueous sub phase). Images were captured by a low geometrical distortion, sensitive, black-white frame transfer CCD camera were transferred in real time to a computer for analysis and use. The images were acquired and analyzed with the Image-Pro Plus 2.1 software (Media Cybernetics, Silver Spring, MD) for maximum resolution.

UV-vis absorption spectrophotometer (Perkin-Elmer Lambda 25) was used for spectroscopic measurement. For absorption measurement the films were kept perpendicular to the incident light and a clean quartz glass slide was used as reference.

The atomic force microscopy (AFM) images of complex film were taken in air with a commercial AFM system Autoprobe M5 (Veeco Instr.) using silicon cantilevers with a sharp, high apex ratio tip (UltraLeversTM, Veeco Instr.). The AFM images presented here were obtained in intermittent-contact ("tapping") mode. Typical scan areas were 3×3 μm^2. The Si wafer substrates were used for the AFM measurements.

RESULTS AND DISCUSSIONS

Adsorption kinetics and complex monolayer formation at the air-water interface :

To check whether SA molecules interact with the DTAB-EY at the air-water interface, surface pressure versus area per molecule isotherm of SA was measured onto pure water and DTAB-EY solution sub phase. Fig. 1 show the surface - pressure vs area per molecule isotherm of SA measured on pure water and DTAB-EY solution (1 : 1 volume ratio of DTAB & EY of concentration 10^{-6} M). The shape and nature of SA isotherm on pure water is consistent with the reported results [30]. However, the SA isotherm measured on DTAB-EY subphase is totally different. Here the isotherm is shifted towards larger area and the collapse pressure is also decreased. This notable change in the SA isotherm measured at DTAB-EY solution sub phase with respect to the same measured at pure water sub phase confirmed that SA interacts with the DTAB-EY molecules at the air-water interface.
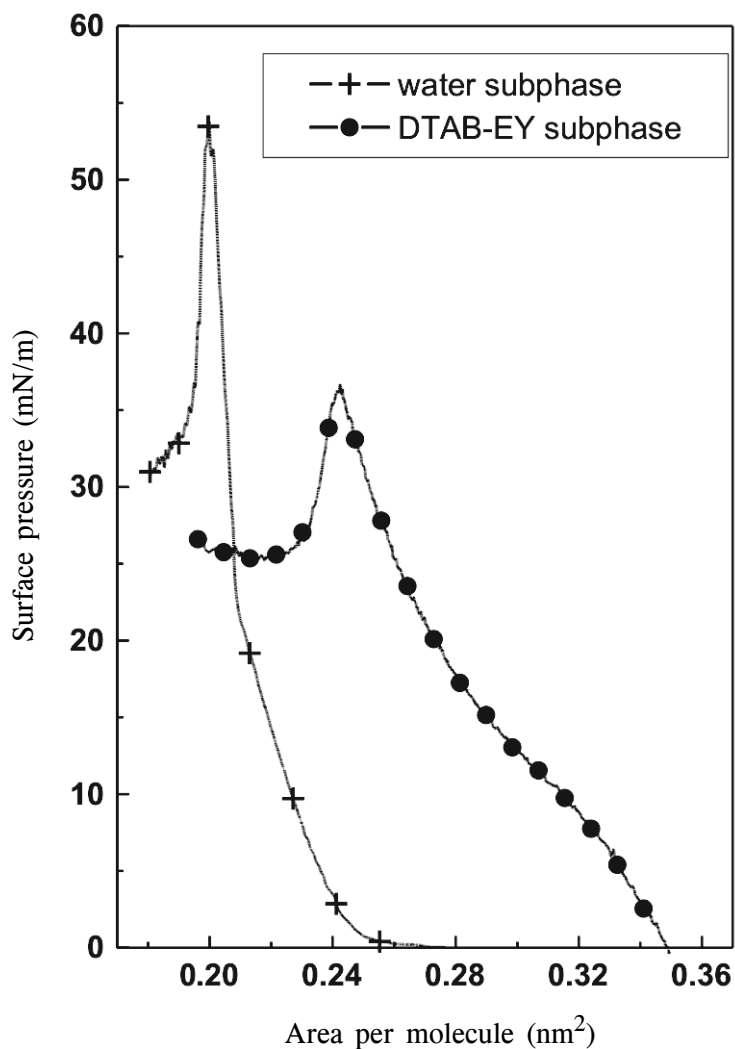
Fig. 1. show the surface - pressure vs area per molecule isotherm of SA measured on pure water and DTAB-EY solution (1 : 1 volume ratio of DTAB & EY of concentration 10^{-6} M) subphase.

Before spreading the SA solution onto DTAB-EY subphase to form SA-DTAB-EY complex film we have checked the change of surface pressure after putting the premixed DTAB-EY aqueous solution in the LB trough and found that surface pressure does not change much with time. The surface pressure varies within 0.4 mN/

m. Before spreading the SA solution on the DTAB-EY subphase the surface pressure was made zero by LB software. Each stability curve was measured more than once and found almost reproducible with a slight variation of the order of 0.5 mN/m.

In order to form a complex monolayer of SA-DTAB-EY at air - water interface, SA solution was spread onto the LB trough filled up with DTAB-EY aqueous solution. Being oppositely charged EY and DTAB interacts with each other. The interaction is mainly electrostatic and hydrophobic resulting in the formation of pre-micellar aggregates. Also interacting with the surface active DTAB, the dye EY are enriched at the interface. The barrier was kept fixed such that the initial surface pressure becomes zero. As soon as the DTAB-EY complex goes close proximity of the floating SA molecules adsorption kinetics starts. A schematic representation of the interaction scheme of DTAB-EY molecules with the SA molecules of the SA monolayer is shown in Fig. 2.

Initially the monolayer was occupied by only the SA molecules. However, with time gradually these SA molecules were replaced by SA-DTAB-EY complex. Finally the whole monolayer was occupied by the complex molecules. The area per molecule of this SA-DTAB-EY complex is greater than that of pure SA molecules. This results a tendency to increase the area per complex molecule in the complex monolayer. However, as the barrier was kept fixed at a particular position, this tendency to increase the area per complex molecule causes an increase in surface pressure. Therefore, surface pressure goes on increasing as the number of complex molecules at air-water interface increases with time. However, the surface pressure becomes stable when all the SA molecules are replaced by the SA-DTAB-EY complex at the air-water interface. This situation is demonstrated by the cartoon (iii) of Fig. 2.

Therefore, the increase in surface pressure with the passage of time is an indication of adsorption kinetics and consequent formation of complex monolayer of SA-DTAB-EY complex molecules at the air-water interface.

It is interesting to mention in this context that there are several reports of complex monolayer formation and monitoring the adsorption kinetics using LB technique [9–11]. Fromherz method was used in order to bring a preformed monolayer of dioctadecyl dimethyl ammonium bromide into contact with the sub phase containing polyelectrolyte to form complex monolayer and to monitor the adsorption kinetics [12, 13]. Similar method was also used by several others to study the protein adsorption [31, 32] onto a preformed monolayer. However the main disadvantage of the process is that during the transfer process, the contact area between the monolayer and the polyelectrolyte solution increases linearly and one can't avoid the possibility of the mixing of sub phase during the transfer of the monolayer. Also there is always a
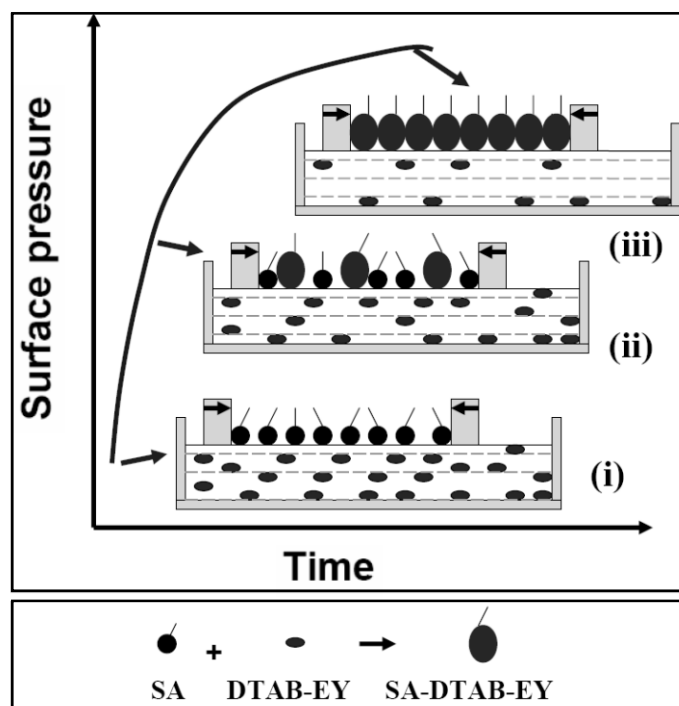
Fig. 2. Schematic representation of the interaction scheme of EY-DTAB complex with the SA molecules at air-water interface in a preformed SA Langmuir monolayer. (i) The LB trough is filled up with aqueous solution of DTAB and EY. SA monolayer onto this sub phase is formed and the barrier is kept fixed at a desired surface pressure. (ii) Surface pressure starts rising due to complex formation (SA + DTAB + EY) at air-water interface in between the barrier. (iii) Surface pressure becomes steady when all the SA molecules in the SA monolayer at the air-water are replaced by SA-DTAB-EY complex.

possibility to change the packing and monolayer morphology during the transfer. Again the transfer speed affects the monolayer stability as a whole. Kawaguchi et al. [11] demonstrated the adsorption of poly (NIPAM) on the preformed pentadecanoic acid (PDA) monolayer. They prepared a monolayer of PDA inside a circular ring shape teflon coated barrier on the LB trough. Then the dilute solution of polyion was injected into the water on the outside of the ring shaped barrier. In our previous efforts [9–10] to adsorb the water soluble material onto preformed Langmuir monolayer, we formed a stearic acid monolayer in the LB trough and the barrier was kept fixed at a desired surface pressure. Then the water soluble material was injected from the back side of the barrier. Our technique was very similar to the Kawaguchi's

technique. Although the possibility of the disturbance of monolayer stability and the mixing of sub phase can be avoided by using this process. However, in this process a concentration gradient of water soluble material is occurred and time dependence of adsorption kinetics cannot be predicted accurately by the steep slope region. To minimize this in the present study we premix the water soluble material in the sub phase uniformly by moving the barrier to and fro several times before spreading the SA solution to form SA monolayer at the interface. Also the position of barrier was noted for zero surface pressure of SA monolayer at the air-water interface by spreading the same amount of SA solution in pure water sub phase. The barrier was kept at that position before spreading the SA solution in DTAB-EY aqueous solution sub phase. This was done in order to measure the exact time dependence of the reaction kinetics. Otherwise there will be some interaction between SA and DTAB-EY during compression of barrier to desired surface pressure.

The adsorption kinetics of SA with the EY doped DTAB molecules are shown in Fig. 3. It was observed that in absence of DTAB and EY molecules SA molecules form stable monolayer at air-water interface. In order to check this, SA solution was spread onto pure water sub phase in LB trough. The barrier was kept fixed to maintain the initial surface pressure at zero. No further increase in surface pressure even after 350 min (curve a in Fig. 3) confirms that SA form stable monolayer at air-water interface. Although there was a fluctuation of surface pressure ± 0.5 mN/m.

Curve b and c in Fig. 3 show the surface pressure versus time graph when SA solution was spread onto LB trough containing DTAB and EY aqueous solution at 50 : 50 and 60 : 40 volume ratio. The concentration of both DTAB and EY was 10^{-6} M. For both the cases the amount of SA solution was kept fixed at 80 μl. The rise in surface pressure indicate the adsorption of the EY doped DTAB molecules in the preformed SA monolayer. It was observed that the surface pressure gradually increased with time and finally became stable and flat. The rate of increase in surface pressure as well as final surface pressure at flat region is higher for higher amount of DTAB. That is the rate of adsorption kinetics increases with the amount of DTAB. We observed that for DTAB amount less than 50% in sub phase did not raise the surface pressure much (Data not shown). Also if the amount of EY was less than 40% then the surface pressure rose faster due to presence of larger amount of DTAB. But in the transferred LB films the presence of EY was very less. This was confirmed by observing very less absorbance for these films (Data not shown).

In our previous works using water soluble N-cetyl N,N,N-trimethyl ammonium bromide (CTAB) doped with rose bengal or congo red [9–10] we observed similar
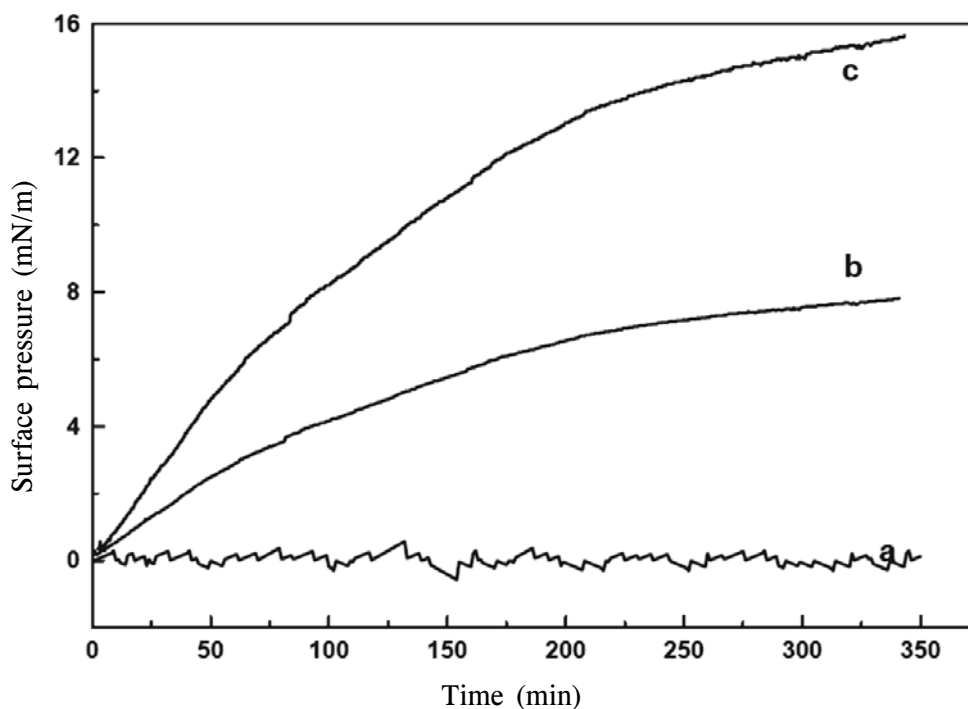
Fig. 3. Surface pressure versus time (π – t) graph of the EY-DTAB-SA complex monolayer at air water interface. In all the cases the spread amount of SA was 80 μl (0.5 mg/ml in chloroform). (a) pure water sub phase in absence of DTAB and EY (b) DTAB + EY (50 : 50 volume ratio) aqueous solution sub phase. (c) DTAB + EY (60 : 40 volume ratio) aqueous solution sub phase. The concentration of constituent DTAB and EY aqueous solutions were 10^{-6} M. In all the cases the starting surface pressure was kept at 0 mN/m.

increase in surface pressure and attainment of flat region at the end of the reaction kinetics due to adsorption of water soluble molecules with the preformed SA Langmuir monolayer. In those works the surface pressure rising were not so uniform and also the surface pressure started rising after few time of spreading. This is because there was a concentration gradient of water soluble molecules as they were injected from the backside of the barrier and it took some time to mix in the sub phase. Also there was a probability of disturbing the SA monolayer during spreading. In the present case to overcome this we prepared the sub phase with DTAB and EY solution and mixed them very well before spreading the SA monolayer. That is why the raise in surface pressure is more uniform and continuous in the present case. There are also

several other molecules like poly (NIPAM) [11], carboxymethyl cellulose sodium salt [12], lysozyme [33], etc. show such initial steep rising and flat plateau like region at the end of the reaction kinetics.

Brewster angle microscopy (BAM) imaging :

To confirm the formation of complex Langmuir monolayer formation at the air-water interface, we have employed traditional in situ imaging technique namely, Brewster angle microscopy (BAM). Fig. 4a and b show the BAM images of pure stearic acid monolayer and SA-DTAB-EY complex monolayer respectively at surface pressure 12 mN/m. BAM image of pure stearic acid monolayer possesses smooth continuous surface with no domain structure. On the other hand discrete aggregated domains are clearly vissible in the BAM (Fig. 4b) image of complex monolayer. These domains are due to the formation complex species in the Langmuir films due to adsorption of water soluble EY and DTAB onto the SA monolayer. The existence of distinct domains of complex species in the complex Langmuir monolayer, provides compelling visual evidence of formation of three component complex Langmuir monolayer at the air - water interface.

Uv-vis absorption spectroscopy :

Fig. 5 shows the UV-Vis absorption spectra of six layer SA-DTAB-EY complex LB film. The films was deposited after completion of the adsorption process i.e. attainment of flat plateau like region in the adsorption kinetics. The sub phase was 50 : 50 volume ratio of DTAB and EY. The EY aqueous solution and microcrystal absorption spectra are also shown in the inset for comparison.

EY aqueous solution absorption spectrum (lower inset of Fig. 5) shows prominent absorption band with peak at 525 nm along with weak high energy band at around 488 nm. The 525 nm band is assigned to be due to the absorption by EY monomer. The small high energy shoulder at 488 nm can be assigned to the $0 \rightarrow 1$ vibronic transition of the monomers and eventually a contribution of H-dimer absorption. This is consistent with the reported literature [34]. On the other hand the microcrystal absorption spectrum shows broadened spectral profile. Also the bands are red shifted with respect to solution absorption spectrum. Here the main absorption peak was observed at 532 nm along with the weak high energy shoulder at 500 nm. These two bands are red shifted by 7 and 12 nm respectively with respect to their solution counterpart. The overall broadening of the spectral profile accompanied with the red shift is due the formation aggregates of EY in the microcrystal. Similar aggregation was also observed for other molecules in microcrystal [35]. The DTAB-EY mixed solution spectra is however very interesting. Here the high energy band
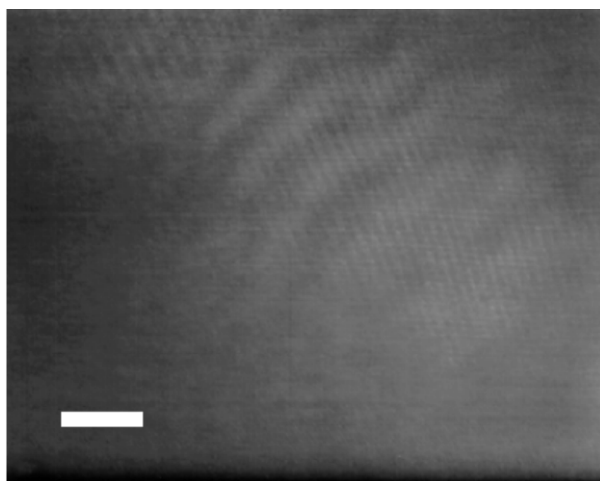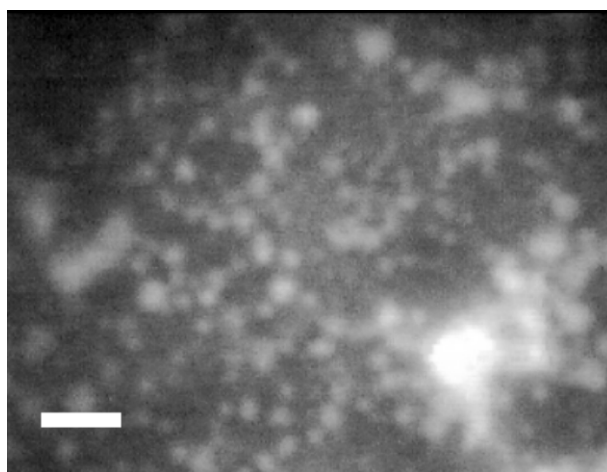
Figure 4a

Figure 4b

Fig. 4. Brewster angle microscopy images of (a) pure stearic acid monolayer and (b) SA-DTAB-EY complex monolayer. Both the image were recorded at 12 mN/m surface pressure. The scale bar represents a length of 250 μm.

is almost indistinguishable and situated at around 500 nm. Also the main absorption peak at 538 nm is red shifted with respect to both EY solution and microcrystal
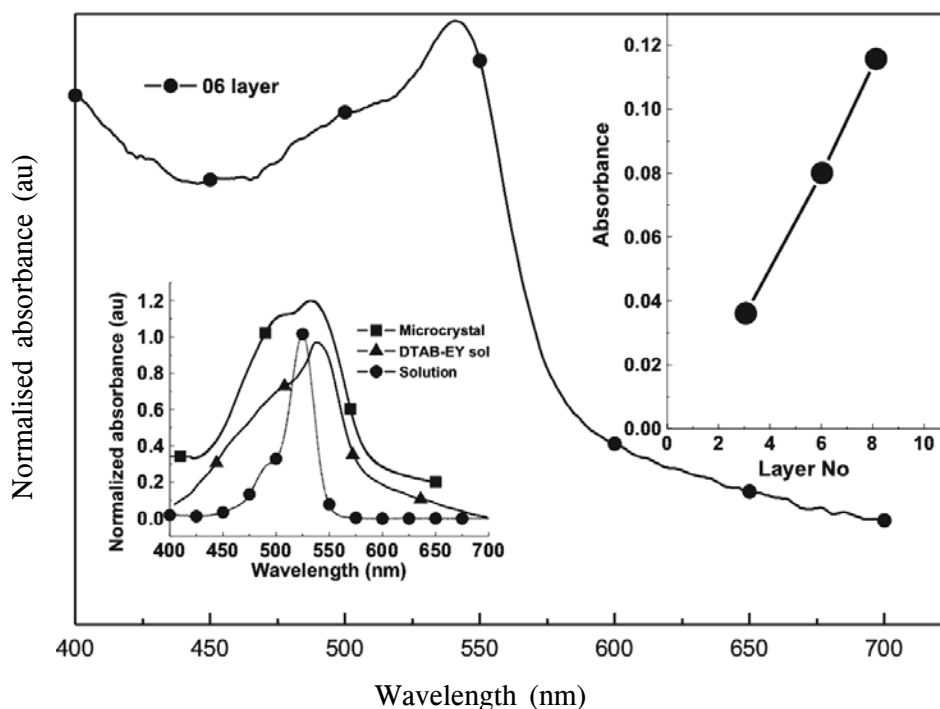
Fig. 5. Normalized UV-Vis absorption spectra of six layer SA-DTAB-EY complex LB films. The LB film was deposited after completion of reaction kinetics i.e. after attainment of the flat plateau region. The sub phase was 50 : 50 volume ratio of DTAB and EY. The plot of absorbance (without normalized) as a function of layer number is shown in upper inset. Lower inset shows the normalized UV-Vis absorption spectra of EY aqueous solution, EY microcrystal and DTAB + EY (50 : 50 volume ratio) mixed solution.

spectrum. Eosin Y is an anionic dye whereas DTAB is a cationic surfactant. When EY is mixed with DTAB, the anionic part of EY interacts with the cationic part of the DTAB molecule and thus forms a electrostatic complex. Due to this interaction the deformation of energy levels occurred in the mixed solution. This deformation results the change in spectral profile for DTAB-EY mixed solution. In one of our previous work we observed such change in spectral profile when rose bengal interacted with CTAB molecules [10].

The absorption spectra of SA-DTAB-EY complex LB film are quite interesting. Here the main absorption peak is at 541 nm which is red shifted by 16 nm and 9 nm with respect to their solution and microcrystal counterpart respectively. Also the

high energy band at 500 nm becomes much broadened. The spectra also show similar spectral profile with the SA-DTAB-EY mixed solution spectrum. Only the difference is that here the extent of red shift of main absorbance is 3 nm more. This may be due to slight change in aggregation when the complex molecules are shifted from solution to the films. With the increase in layer number the spectral profile remains almost similar except an increase in absorbance. The plot of absorbance as a function of layer number (inset of Fig. 5) shows the linear growth of the EY in the LB films with increasing layer number.

Atomic force microscopy of SA-DTAB-EY complex film :

The morphology and thickness of the SA-DTAB-EY complex LB films were investigated by AFM studies. Fig. 6 shows a representative image along with the height profile. Also the same image in 3D view has been presented. The AFM image shows that the film contains different size nano dimensional domains of SA-DTAB-EY complex molecules. The maximum height of the few domains is in the 6-8 nm
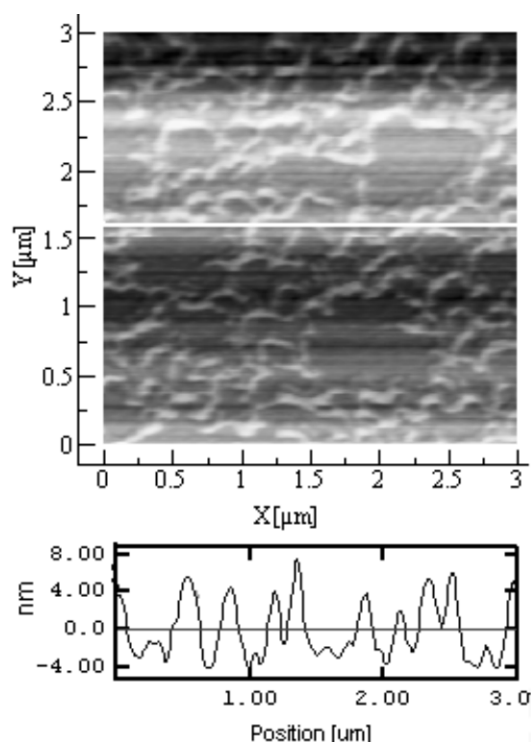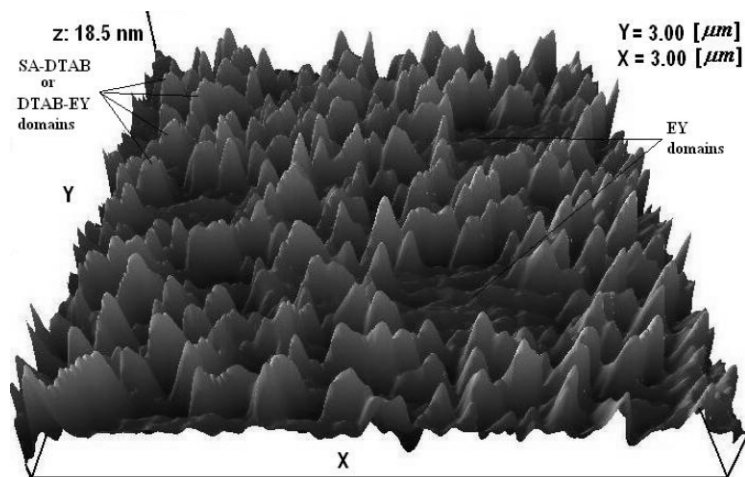

Figure 6a

Figure 6b

Fig. 6. (a) Topographic AFM image of SA-DTAB-EY complex LB film deposited onto a silicon wafer substrate after completion of reaction kinetics along with the thickness profile across the line in the image. (b) Three dimensional view of the same image.

range. However some domain with lower height is also observed. The difference in shape and size of the domains are mainly due to the different extent of interaction among SA, DTAB and EY molecules, resulting in the presence of different species in the complex LB films. EY molecules interact with the DTAB molecules in water and form complex. These DTAB-EY complex molecules interact with the SA molecules in the floating monolayer and consequently form SA-DTAB-EY complex. Again SA interacts with the DTAB molecules being opposite polarity. Therefore in the LB films DTAB-EY complex is formed and stacked as well as some EY molecules are detached from the DTAB molecules, while DTAB molecules form complex with SA molecules and within the organization of DTAB-SA complex molecules EY molecules may get stacked and form microcrystalline aggregates. Therefore in the complex films may consist of nano dimensional aggregate of DTAB-EY, EY as well as SA-DTAB complex species. Fig. 7 represent the modified schematic diagram of the complex monolayer.
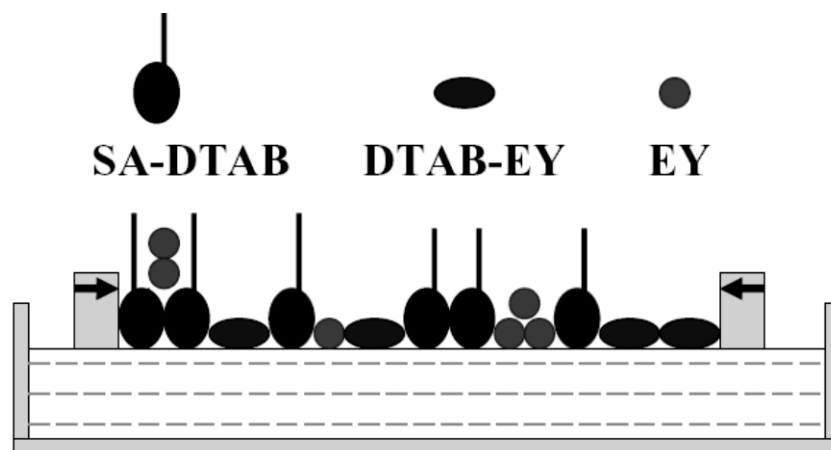
Fig. 7. Modified schematic diagram of the complex monolayer at air - water interface.

CONCLUSION

In the present study we have demonstrated the incorporation of water soluble eosin Y (EY) in complex LB films. This was done by electrostatic and hydrophobic interaction between water soluble dodecyl trimethyl ammonium bromide (DTAB) and EY and consequent adsorption of the DTAB-EY complex onto a floating SA monolayer. The adsorption kinetics and complex monolayer formation was confirmed by monitoring the increase in surface pressure with time (π–t curve) at air - water interface. The π–t curves initially show steep rising and become flat showing plateau like region at the end of the adsorption kinetics, indicating the completion of the adsorption process. It was observed that more than 300 minutes were required to complete the reaction kinetics. BAM image reveals formation of distinct domains in the complex Langmuir films and provides visual evidence on complex film formation at air-water interface. The EY monomer (0 $\rightarrow$ 0) absorption bands in complex LB film was red shifted with respect to pure EY aqueous solution and microcrystal absorption spectrum. Also overall broadening of spectral profile was observed for complex LB film spectrum. The linear increase in EY absorbance with layer number in complex LB films confirms the successful incorporation of EY in LB films. AFM investigation of SA-DTAB-EY complex film shows the presence of domains with different size and height in the complex LB films.

ACKNOWLEDGEMENT

REFERENCES

1. I. Langmuir, *J. Am. Chem. Soc.*, 39, 1848 (1917).

2. K. B. Blodgett, *J. Am. Chem. Soc.*, 57, 1007 (1935).

3. A. Ulman, '*An Introduction to Ultrathin Organic Films : From Langmuir – Blodgett Films to Self Assemblies*', Academic Press, New York, (1991).

4. M. C. Petty, '*Langmuir – Blodgett Films : An Introduction*', Cambridge University Press, Cambridge, (1996).

5. S. A. Hussain, P. K. Paul, D. Bhattacharjee, *J. Phys. Chem. Solids.*, 67, 2542 (2006).

6. S. A. Hussain, D. Bhattacharjee, *Modern Phys. Letts., B,* 23 (27), 3437. (2009).

7. G. G. Roberts, '*Langmuir – Blodgett Films*' ; Plenum Press, New York, (1990).

8. D. R. Talham, T. Yamamoto, M. W. Meisel, *J. Phys: Condens. Matter.,* 20, 184006 (2008).

9. S. Biswas, S.A. Hussain, S. Deb, R. K. Nath, D. Bhattacharjee, *Spectrochim. Acta A,* 65, 628 (2006).

10. S. Biswas, D. Bhattacharjee, R. K. Nath, S. A. Hussain, *J. Colloid Interface Sci.*, 311, 361 (2007).

11. M. Kawaguchi, M. Yamamoto, T. Kato, *Langmuir,* 14, 2582 (1998).

12. J. Engelking, H. Menzel, *Eur. Phys. J. E.*, 5, 87 (2001).

13. J. Engelking, D. Ulbrich, H. Menzel, *Macromolecules*, 33, 9026 (2000).

14. D. Vollhardt, V. Melzer, *J. Phys. Chem. B,* 101, 3370 (1997).

15. D. Vollhardt, V. Melzer, V. Fainerman, *Thin Solid Films,* 327, 842 (1998).

16. D. Vollhardt, *Adv. Colloid Surface Sci.,* 79, 19 (1999).

17. N. J. Armstrong, K. Chari, T. L. Penner, *J. Colloid Interface Sci.,* 183, 617 (1996).

18. V. Rosilio, M. M. Boissonnade, J. Zhang, L. Jiang, A. Baszkin, *Langmuir,* 13, 4669 (1997).

19. T. R. Baekmark, G. Elender, D. D. Lasic, E. Sackmann, *Langmuir,* 11, 3975 (1995).

20. L. H. Lee, '*Adhesion and Adsorption of polymers*', Plenum Press, New York, (1980).

21. D. H. Napper, *'Polymer Stabilization of Colloid Dispersions'*, Academic Press, London, (1975).

22. E. Ruckenstein, D. B. Chang, *J. Colloid Interface Sci.*, 123, 170 (1988).

23. M. Antonietti, C. Burger, A. Thunemann, *Trends Polym. Sci.,* 5, 262 (1997).

24. C. K. Ober, G. Wegner, *Adv. Mater.,* 9, 17 (1997).

25. S. Zhou, B. Chu, *Adv. Mater.,* 12, 54 (2000).

26. J. D. Pitts, A. R. Howell, R. Taboada, I. Banerjee, J. Wang, S. L. Goodman, P. J. Campagnol, *Photochem. Photobio.,* 76(2), 135 (2002).

27. S. –S. Kim, J. H. Yum, Y. E. Sung, *Solar Energy Materials & Solar Cells,* 79, 495 (2003).

28. V. M. Guerin, C. Magne, Th. Pauporté, T. Le Bahers, J. Rathousky, *ACS applied materials and interfaces,* 2(12), 3677 (2010).

29. M. Lessard-Viger, M. Rioux, L. Rainville, D. Boudreau, *Nano Lett.,* 9(8), 3066 (2009).

30. A. Hussain, P. K. Paul, D. Bhattacharjee *J. Colloid Interface Sci.,* 299, 785 (2006).

31. P. Fromherz, *Biochim Biophys. Acta,* 225, 382 (1971).

32. F. Ebler, Dissertation, *Universitat Mainz,* (1998).

33. S. Sundaram, J. K. Ferri, D. Vollhardt, K. J. Stebe, *Langmuir,* 14, 1208 (1998).

34. C. Li, S. Liu, Z. Liu, X. Hu, *J. Fluoresc.,* 21 (2), 723 (2011).

35. S. Deb, S. Biswas, S. A. Hussain, D. Bhattacharjee, *Chem. Phys. Letts.,* 405, 323 (2005).